Title
Cloaking a sensor for three-dimensional Maxwell's equations: transformation optics approach

Journal
Optics Express, 19(21)

ISSN
1094-4087

Authors
Chen, Xudong
Uhlmann, Gunther

Publication Date
2011-10-03

DOI
10.1364/OE.19.020518

Cloaking a sensor for three-dimensional Maxwell's equations: transformation optics approach

Xudong Chen[1,*] **and Gunther Uhlmann**[2,3]

[1]*Department of Electrical and Computer Engineering, National University of Singapore, 117576 Singapore*
[2]*Department of Mathematics, University of California at Irvine, Irvine, CA 92697, USA*
[3]*Department of Mathematics, University of Washington, Seattle, WA 98195, USA*
[*]*elechenx@nus.edu.sg*

Abstract: The ideal transformation optics cloaking is accompanied by shielding: external observations do not provide any indication of the presence of a cloaked object, nor is any information about the fields outside detectable inside the cloaked region. In this paper, a transformation is proposed to cloak three-dimensional objects for electromagnetic waves in sensor mode, i.e., cloaking accompanied by degraded shielding. The proposed transformation tackles the difficulty caused by the fact that the lowest multipole in three-dimensional electromagnetic radiation is dipole rather than monopole. The loss of the surface impedance of the sensor plays an important role in determining the cloaking modes: ideal cloaking, sensor cloaking and resonance.

OCIS codes: (260.2710) Inhomogeneous optical media; (260.2110) Electromagnetic theory; (160.1190) Anisotropic optical materials; (290.3200) Inverse scattering.

References and links

1. J. B. Pendry, D. Schurig, and D. R. Smith, "Controlling electromagnetic fields," Science **312**, 1780–1782 (2006).
2. A. Greenleaf, M. Lassas, and G. Uhlmann, "Anisotropic conductivities that cannot be detected by EIT," Physiol. Measure. **24**, 413–419 (2003).
3. Y. Luo, H. S. Chen, J. J. Zhang, L. X. Ran, and J. A. Kong, "Design and analytical full-wave validation of the invisibility cloaks, concentrators, and field rotators created with a general class of transformations," Phys. Rev. B **77**, 125127 (2008).
4. A. Greenleaf, Y. Kurylev, M. Lassas, and G. Uhlmann, "Full-wave invisibility of active devices at all frequencies," Commun. Math. Phys. **275**, 749–789 (2007).
5. B. L. Zhang, H. S. Chen, B. I. Wu, and J. A. Kong, "Extraordinary surface voltage effect in the invisibility cloak with an active device inside," Phys. Rev. Lett. **100**, 063904 (2008).
6. H. Chen, C. T. Chan, and P. Sheng, "Transformation optics and metamaterials," Nat. Mater. **9**, 387–396 (2010).
7. H. Chen, X. Luo, H. Ma, and C. T. Chan, "The anti-cloak," Opt. Express **16**, 14603–14608 (2008).
8. B. L. Zhang, Y. Luo, X. G. Liu, and G. Barbastathis, "Macroscopic invisibility cloak for visible light," Phys. Rev. Lett. **106**, 033901 (2011).
9. W. X. Jiang, T. J. Cui, G. X. Yu, X. Q. Lin, Q. Cheng, and J. Y. Chin, "Arbitrarily elliptical-cylindrical invisible cloaking," J. Phys. D: Appl. Phys. **41**, 085504 (2008).
10. A. Alù and N. Engheta, "Cloaking a sensor," Phys. Rev. Lett. **102**, 233901 (2009).
11. A. Alù and N. Engheta, "Cloaked near-field scanning optical microscope tip for noninvasive near-field imaging," Phys. Rev. Lett. **105**, 263906 (2010).
12. A. Greenleaf, Y. Kurylev, M. Lassas, and G. Uhlmann, "Cloaking a sensor via transformation optics," Phys. Rev. E **83**, 016603 (2011).

#151762 - $15.00 USD Received 27 Jul 2011; revised 7 Sep 2011; accepted 9 Sep 2011; published 3 Oct 2011

13. G. Castaldi, I. Gallina, V. Galdi, A. Alù, and N. Engheta, "Cloak/anti-cloak interactions," Opt. Express **17**, 106343 (2009).
14. G. Castaldi, I. Gallina, V. Galdi, A. Alù, and N. Engheta, "Analytical study of spherical cloak/anti-cloak interactions," Wave Motion **48**, 455–467 (2011).
15. Y.-L. Geng, C.-W. Qiu, and N. Yuan, "Exact solution to electromagnetic scattering by an impedance sphere coated with a uniaxial anisotropic layer," IEEE Trans. Antennas Propagat. **57**, 572–576 (2009).
16. M. Abramowitz and I. A. Stegun, *Handbook of Mathematical Functions with Formulas, Graphs, and Mathematical Tables* (Dover, New York, 1972).
17. D. Schurig, J. B. Pendry, and D. R. Smith, "Calculation of material properties and ray tracing in transformation media," Opt. Express **14**, 9794–9804 (2006).

1. Introduction

Transformation optics has been a popular research topic in the past few years due to its exciting property of designing cloaks which can completely hide objects from electromagnetic detection. The fundamental idea is the invariance of Maxwell's equations under a space-deforming transformation if the material properties are altered accordingly [1–9]. However, the ideal cloaking is accompanied by shielding: There is a decoupling of the fields inside and outside of the cloaked region, so that external observations do not provide any indication of the presence of a cloaked object, nor is any information about the fields outside detectable inside the cloaked region. In many real-world applications, however, there are needs for effectively cloaking sensors and detectors so that their presence may be less disturbing to the surrounding environment. For example, in a receiving antenna array, we aim at reducing the coupling among antenna elements so that an element is able to receive electromagnetic signal without disturbing the field received by other elements. When the near-field scanning optical microscope (NSOM) operates in collection mode, the tip should be very close to the scattering objects, which inevitably yields undesired multiple scattering between tip and scatterer and thus degrades the accuracy of the measured field.

In the past few years, there have been attempts to design sensors that are able to perceive electromagnetic radiation and at the same time have negligible disturbance to the surrounding environment, which is referred to as 'cloaking sensors' or 'cloak in sensor mode'. The first paper in this direction is [10], where a plasmonic coating allows electromagnetic wave to reach the sensor and at the same time the scattering due to the sensor is canceled out by that of the cloak. The idea has been applied to cloak a NSOM tip for the purpose of near field imaging [11], which is of great industrial and scientific significance. However, there are also some limitations of the method. For example, it can only cloak sensors smaller or comparable to wavelength and the shape and material of the cloak depend on the geometrical and physical properties of the sensor. Another approach to cloak a sensor is transformation optics. In [12], a sensor that is cladded with a sphere with surface impedance is placed inside the cloak. This method works for sensors of arbitrary size and shape as long as the sensors are able to measure the field at the boundary of the cladding sphere. As mentioned in [12], this transformation optics approach is able to achieve in cloaking a sensor for acoustic waves and two-dimensional (2D) electromagnetic waves. However, a further calculation shows that the transformation optics approach proposed in [12] cannot cloak a sensor for three-dimensional (3D) electromagnetic waves. This is mainly due to the fact that the lowest multipole in 3D electromagnetic radiation is dipole rather than monopole. The asymptotic behavior, for small arguments, of Riccati-Bessel functions of order one and above leads to vanishing electromagnetic fields inside the cloak, i.e., the shielding effect is still hand in hand with the cloaking effect. Another transformation optics approach is presented in [13, 14], where both a cloak layer and an anti-cloak layer play the role to achieve cloaking sensor effect. Whereas this approach can cloak sensors of arbitrary size and works for both 2D and 3D electromagnetic waves, the sensor is modeled as a dielectric sphere

#151762 - $15.00 USD Received 27 Jul 2011; revised 7 Sep 2011; accepted 9 Sep 2011; published 3 Oct 2011

and the papers do not discuss whether the method works for a generic sensor, i.e., whether both the cloak layer and anti-cloak layer depend on the shape and material of the sensor. In addition, the cloaking device consists of five layers, eight unknowns for each order of multipole, and two small parameters to be adjusted, which makes it tedious to derive analytical solutions.

In this paper, we propose a novel transformation optics method to cloak a sensor, which can be of arbitrary size, shape, and material, for 3D electromagnetic waves. The cloaking device consists in three layers, five unknowns for each order of multipole, and one small parameter to be adjusted. Analytical results can be obtained for each of five unknowns even without resource to small parameter approximation. Compared with [12], the proposed transformation, from the physical space to the virtual space, circumvents the difficulty caused by the fact that the lowest multipole in 3D electromagnetic radiation is dipole rather than monopole. The loss of the surface impedance of the sensor plays an important role in determining the cloaking modes: ideal cloaking, sensor cloaking and resonance. Numerical simulations validate the proposed transformation model.

2. Configuration of the cloak and the sensor

As shown in Fig. 1. The sensor is placed inside a sphere of radius R_0, with surface impedance boundary condition $-E_\theta/H_\phi = E_\phi/H_\theta = \alpha_0$ (see [15] and references therein). The sensor is able to measure the tangential electric fields at the surface of the sphere.The cloak layer is within an annulus with inner and outer radii R_1 and R_2, respectively. All three spheres mentioned above are concentric, with the center being the origin of the coordinate system in the physical space. The space between spheres of radii R_0 and R_1, as well as the space outside of the sphere of radius R_2, are free space. The permittivity and permeability of the cloak layer are obtained using

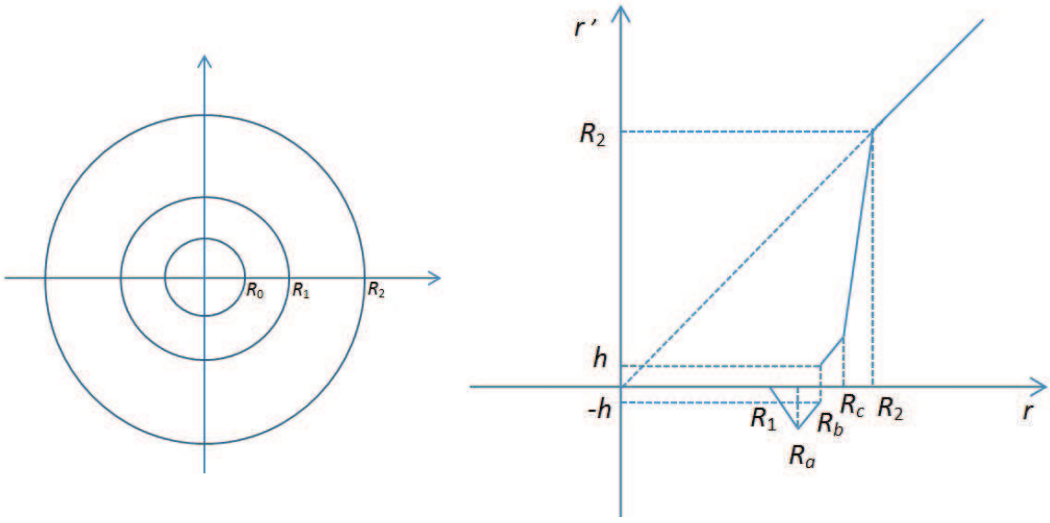

(a) (b)

Fig. 1. The geometry of the sensor and the transformation function. (a) A sensor of arbitrary shape is placed inside a sphere with radius R_0 and surface impedance α_0, and it is able to measure the tangential electric field on the spherical surface. The cloak layer is in between spheres of radii $R_1+\delta$ and R_2, where δ is an small positive number and is not shown in the figure due to its small magnitude. Other regions are free space. (b) The transformation $r' = f(r)$ from the physical space to the virtual space.

#151762 - $15.00 USD Received 27 Jul 2011; revised 7 Sep 2011; accepted 9 Sep 2011; published 3 Oct 2011

the invariance of Maxwell's equations under transformation of the spatial coordinate systems. Consider a coordinate transformation between the virtual space (curved free space) with the physical space. The former has spatial coordinates r', θ', ϕ', permittivity ε_0, and permeability μ_0, whereas the latter has spatial coordinates r, θ, ϕ, and parameters $\overline{\overline{\varepsilon}}, \overline{\overline{\mu}}$. The transformation is only in the radial direction, i.e.,

$$r' = f(r), \quad \theta' = \theta, \quad \phi' = \phi. \tag{1}$$

The associated permittivity and permeability tensors are given by

$$\overline{\overline{\varepsilon}} = \varepsilon_r(r)\hat{r}\hat{r} + \varepsilon_t(r)\hat{\theta}\hat{\theta} + \varepsilon_t(r)\hat{\phi}\hat{\phi} \tag{2}$$

$$\overline{\overline{\mu}} = \mu_r(r)\hat{r}\hat{r} + \mu_t(r)\hat{\theta}\hat{\theta} + \mu_t(r)\hat{\phi}\hat{\phi}, \tag{3}$$

where

$$\varepsilon_r = \varepsilon_0 \frac{f^2(r)}{r^2 f'(r)}, \quad \varepsilon_t = \varepsilon_0 f'(r) \tag{4}$$

$$\mu_r = \mu_0 \frac{f^2(r)}{r^2 f'(r)}, \quad \mu_t = \mu_0 f'(r). \tag{5}$$

It is well known that the transform that satisfies both $f(R_1) = 0$ and $f(R_2) = R_2$ yields perfect invisibility. To avoid singularities, we let the boundary of the inner cloaking material be at $R_1 + \delta$, where δ is a small positive number. The incident wave is generated by a time-harmonic $[\exp(-\mathrm{i}\omega t)]$ source that is located outside of the sphere of radius R_2. To achieve cloaking a sensor, we aim at obtaining a negligible scattered field outside of the sphere of radius R_2 and at the same time perceivable electromagnetic field at the surface of the cladding sphere.

3. Analytical results for electromagnetic fields

Electromagnetic fields can be decomposed into two independent modes, TE and TM modes (transverse to radial direction in spherical coordinate system), which are dual to each other. For the TM mode, the **B** field can be expressed as

$$\mathbf{B} = \nabla \times \left(\hat{r} f' \Phi_M\right), \tag{6}$$

where the scalar potential Φ_M satisfies

$$\frac{1}{f^2 \sin\theta}\left[\frac{\partial}{\partial\theta}\left(\sin\theta \frac{\partial \Phi_M}{\partial\theta}\right) + \frac{1}{\sin\theta}\frac{\partial^2 \Phi_M}{\partial\phi^2}\right] + \frac{\partial^2 \Phi_M}{\partial f^2} + k_0^2 \Phi_M = 0, \tag{7}$$

where $k_0^2 = \omega^2 \varepsilon_0 \mu_0$. Separation of variables yields

$$\Phi_M = \sum_{n=1}^{N} \sum_{m=-n}^{n} A_{nm} \hat{B}_n(k_0 f) Y_n^m(\theta, \phi), \tag{8}$$

where N is the highest order multipole used in the numerical simulations, $\hat{B}_n(z) = z b_n(z)$ is the Riccati-Bessel function, and Y_n^m are spherical harmonics. Now the magnetic field **H** and the electric field **E** can be expressed as

$$\mathbf{H} = \mu_0^{-1} \frac{1}{r\sin\theta}\frac{\partial \Phi_M}{\partial\phi}\hat{\theta} - \mu_0^{-1}\frac{1}{r}\frac{\partial \Phi_M}{\partial\theta}\hat{\phi} \tag{9}$$

$$\mathbf{E} = \frac{\mu_0^{-1}\varepsilon_0^{-1}}{-\mathrm{i}\omega}\left[f'\left(\frac{\partial^2 \Phi_M}{\partial f^2} + k_0^2 \Phi_M\right)\hat{r} + \frac{1}{r}\frac{\partial^2 \Phi_M}{\partial f \partial\theta}\hat{\theta} + \frac{1}{r\sin\theta}\frac{\partial^2 \Phi_M}{\partial f \partial\phi}\hat{\phi}\right]. \tag{10}$$

#151762 - $15.00 USD Received 27 Jul 2011; revised 7 Sep 2011; accepted 9 Sep 2011; published 3 Oct 2011

The potential Φ_M in the three regions is written as

$$\Phi_M^{\rm ext}(r,\theta,\phi) = \sum_n\sum_m \left[K_{nm}\hat{J}_n(k_0 r)+A_{nm}\hat{H}_n^{(1)}(k_0 r)\right]Y_n^m(\theta,\phi),\ \text{for } r>R_2 \quad (11)$$

$$\Phi_M^{\rm clo}(r,\theta,\phi) = \sum_n\sum_m \left[B_{nm}\hat{J}_n(k_0 f)+C_{nm}\hat{H}_n^{(1)}(k_0 f)\right]Y_n^m(\theta,\phi),\ \text{for } R_1+\delta<r<R_2 \quad (12)$$

$$\Phi_M^{\rm int}(r,\theta,\phi) = \sum_n\sum_m \left[D_{nm}\hat{J}_n(k_0 r)+E_{nm}\hat{H}_n^{(1)}(k_0 r)\right]Y_n^m(\theta,\phi),\ \text{for } R_0<r<R_1+\delta. \quad (13)$$

Since the source is given, K_{nm} is uniquely determined. For each multipole of order n, we will solve for five unknows A_{nm}, B_{nm}, C_{nm}, D_{nm}, and E_{nm}. Eqs. (9) and (10) indicate that the continuities of tangential components of $\mathbf{H}$ and $\mathbf{E}$ across the boundaries $r=R_1+\delta$ and $r=R_2$ amount to the continuities of Φ_M and $\frac{\partial\Phi_M}{\partial(k_0 f)}$, respectively. The impedance boundary condition reduces to $\frac{\partial\Phi_M}{\partial(k_0 f)}-\alpha\Phi_M=0$, where α is proportional to α_0. Thus, we have the following boundary conditions

$$B_{nm}\hat{J}_n(k_0R_2)+C_{nm}\hat{H}_n^{(1)}(k_0R_2) = K_{nm}\hat{J}_n(k_0R_2)+A_{nm}\hat{H}_n^{(1)}(k_0R_2) \quad (14)$$

$$B_{nm}\hat{J}_n'(k_0R_2)+C_{nm}\hat{H}_n^{(1)\prime}(k_0R_2) = K_{nm}\hat{J}_n'(k_0R_2)+A_{nm}\hat{H}_n^{(1)\prime}(k_0R_2) \quad (15)$$

$$B_{nm}\hat{J}_n(k_0f(R_1+\delta))+C_{nm}\hat{H}_n^{(1)}(k_0f(R_1+\delta)) = D_{nm}\hat{J}_n(k_0(R_1+\delta))+E_{nm}\hat{H}_n^{(1)}(k_0(R_1+\delta)) \quad (16)$$

$$B_{nm}\hat{J}_n'(k_0f(R_1+\delta))+C_{nm}\hat{H}_n^{(1)\prime}(k_0f(R_1+\delta)) = D_{nm}\hat{J}_n'(k_0(R_1+\delta))+E_{nm}\hat{H}_n^{(1)\prime}(k_0(R_1+\delta)) \quad (17)$$

$$D_{nm}\hat{J}_n'(k_0R_0)+E_{nm}\hat{H}_n^{(1)\prime}(k_0R_0) = \alpha\left[D_{nm}\hat{J}_n(k_0R_0)+E_{nm}\hat{H}_n^{(1)}(k_0R_0)\right]. \quad (18)$$

It is easy to see that Eqs. (14) and (15) yield $B_{nm}=K_{nm}$ and $A_{nm}=C_{nm}$. There are two cases for Eq. (18).

3.1. Case 1

When $\hat{J}_n'(k_0R_0)-\alpha\hat{J}_n(k_0R_0)\neq 0$, we have

$$D_{nm}=-\frac{\hat{H}_n^{(1)\prime}(k_0R_0)-\alpha\hat{H}_n^{(1)}(k_0R_0)}{\hat{J}_n'(k_0R_0)-\alpha\hat{J}_n(k_0R_0)}E_{nm}\equiv g(\alpha)E_{nm} \quad (19)$$

Now we solve for two unknowns A_{nm} and E_{nm} from two linear equations,

$$K_{nm}\hat{J}_n(k_0f(R_1+\delta))+A_{nm}\hat{H}_n^{(1)}(k_0f(R_1+\delta)) = E_{nm}\left[g(\alpha)\hat{J}_n(k_0(R_1+\delta))+\hat{H}_n^{(1)}(k_0(R_1+\delta))\right] \quad (20)$$

$$K_{nm}\hat{J}_n'(k_0f(R_1+\delta))+A_{nm}\hat{H}_n^{(1)\prime}(k_0f(R_1+\delta)) = E_{nm}\left[g(\alpha)\hat{J}_n'(k_0(R_1+\delta))+\hat{H}_n^{(1)\prime}(k_0(R_1+\delta))\right] \quad (21)$$

We obtain:

$$E_{nm}/K_{nm}=i/F_n, \quad (22)$$

$$A_{nm}/K_{nm}=G_n/F_n, \quad (23)$$

where

$$\begin{aligned} F_n = {} & \left[g\hat{J}_n(k_0(R_1+\delta))+\hat{H}_n^{(1)}(k_0(R_1+\delta))\right]\hat{H}_n^{(1)\prime}(k_0f(R_1+\delta)) \\ & -\left[g\hat{J}_n'(k_0(R_1+\delta))+\hat{H}_n^{(1)\prime}(k_0(R_1+\delta))\right]\hat{H}_n^{(1)}(k_0f(R_1+\delta)) \end{aligned} \quad (24)$$

$$\begin{aligned} G_n = {} & -\left[g\hat{J}_n(k_0(R_1+\delta))+\hat{H}_n^{(1)}(k_0(R_1+\delta))\right]\hat{J}_n'(k_0f(R_1+\delta)) \\ & +\left[g\hat{J}_n'(k_0(R_1+\delta))+\hat{H}_n^{(1)\prime}(k_0(R_1+\delta))\right]\hat{J}_n(k_0f(R_1+\delta)) \end{aligned} \quad (25)$$

#151762 - $15.00 USD Received 27 Jul 2011; revised 7 Sep 2011; accepted 9 Sep 2011; published 3 Oct 2011

and the Wronskian $\hat{J}_n\hat{H}_n^{(1)\prime} - \hat{J}_n'\hat{H}_n^{(1)} = i$ is used.

It is worth highlighting that we have obtained analytical result for E_{nm} without using any approximation. From here onwards, we will use the fact that δ is a small parameter to simplify the obtained analytical result. For an infinitesimal parameter z, we have the asymptotics $\hat{J}_n(z) \approx p_n z^{n+1}$ and $\hat{H}_n^{(1)}(z) \approx q_n z^{-n}$ [16]. Using Taylor's expansion and the fact that $f(R_1) = 0$, we obtain

$$\begin{aligned} F_n &\approx \left\{ g\hat{J}_n(k_0R_1) + \hat{H}_n^{(1)}(k_0R_1) + k_0\delta\left[g\hat{J}_n'(k_0R_1) + \hat{H}_n^{(1)\prime}(k_0R_1)\right] + \frac{(k_0\delta)^2}{2}\left[g\hat{J}_n''(k_0R_1) + \hat{H}_n^{(1)\prime\prime}(k_0R_1)\right]\right\} \\ &\quad \times(-nq_n)\left[k_0 f(R_1+\delta)\right]^{-(n+1)} \\ &\quad -\left\{g\hat{J}_n'(k_0R_1) + \hat{H}_n^{(1)\prime}(k_0R_1) + k_0\delta\left[g\hat{J}_n''(k_0R_1) + \hat{H}_n^{(1)\prime\prime}(k_0R_1)\right] + O(\delta^2)\right\} q_n\left[k_0 f(R_1+\delta)\right]^{-n} \\ &= q_n\left[k_0 f(R_1+\delta)\right]^{-(n+1)}(A_1+A_2+A_3+A_4+A_5+A_6), \end{aligned} \tag{26}$$

where

$$A_1 = -n\left[g\hat{J}_n(k_0R_1) + \hat{H}_n^{(1)}(k_0R_1)\right], \tag{27}$$

$$A_2 = -nk_0\delta\left[g\hat{J}_n'(k_0R_1) + \hat{H}_n^{(1)\prime}(k_0R_1)\right], \tag{28}$$

$$A_3 = -k_0 f(R_1+\delta)\left[g\hat{J}_n'(k_0R_1) + \hat{H}_n^{(1)\prime}(k_0R_1)\right], \tag{29}$$

$$A_4 = -k_0 f(R_1+\delta)k_0\delta\left[g\hat{J}_n''(k_0R_1) + \hat{H}_n^{(1)\prime\prime}(k_0R_1)\right], \tag{30}$$

$$A_5 = -n\frac{(k_0\delta)^2}{2}\left[g\hat{J}_n''(k_0R_1) + \hat{H}_n^{(1)\prime\prime}(k_0R_1)\right], \tag{31}$$

$$A_6 = O(\delta^2) f(R_1+\delta), \tag{32}$$

where the Landau big-o notation $O(\cdot)$ denotes terms of the same order, i.e., neglecting constant multipliers and higher-order terms. Depending on whether or not the leading term in F_n is zero, we discuss the two following two cases.

3.1.1. Case 1.1

When $g\hat{J}_n(k_0R_1) + \hat{H}_n^1(k_0R_1) \neq 0$,

$$\frac{E_{nm}}{K_{nm}} = \mathrm{i}q_n^{-1}\left[k_0 f(R_1+\delta)\right]^{n+1} A_1^{-1}. \tag{33}$$

To further quantify the asymptotic behavior of E_{nm}, we can express the transform function $f(R_1+\delta)$ as, considering the fact that $f(R_1) = 0$ and δ is small,

$$f(R_1+\delta) = \beta\delta^s + o(\delta^s), \tag{34}$$

for some β and s, where $s > 0$. Note that the Landau little-o notation $o(\cdot)$ denotes higher order terms, i.e., those approaching to zero at faster rates. Thus,

$$\frac{E_{nm}}{K_{nm}} = O(\delta^{(n+1)s}). \tag{35}$$

From Eq. (23), a straightforward calculation gives that $A_{nm} = O(\delta^{(2n+1)s})$. Since $n \geq 1$, we see both E_{nm} and A_{nm} approach zero as δ approaches zero, indicating that cloaking effect is coupled with shielding effect, i.e., there is no sensor effect.

#151762 - $15.00 USD Received 27 Jul 2011; revised 7 Sep 2011; accepted 9 Sep 2011; published 3 Oct 2011

3.1.2. Case 1.2

When $g\hat{J}_n(k_0R_1)+\hat{H}_n^{(1)}(k_0R_1)=0$, the Wronskian $\hat{J}_n\hat{H}_n^{(1)\prime}-\hat{J}_n'\hat{H}_n^{(1)}=i$ implies that $g\hat{J}_n'(k_0R_1)+\hat{H}_n^{(1)\prime}(k_0R_1)\neq 0$. It is also important to stress that the differentiation of the Wronskian with respect to k_0R_1 yields $g\hat{J}_n''(k_0R_1)+\hat{H}_n^{(1)\prime\prime}(k_0R_1)=0$. Subsequently, we see from Eq. (28) to Eq. (31) that, $A_2\neq 0$, $A_3\neq 0$, and $A_4=A_5=0$. Due to the presence of a nonzero A_3, F_n contains a term of order $O(\delta^{-ns})$, which is infinite and eventually leads to zero value of E_{nm} as δ goes to zero. In this case, there is no sensing effect. To achieve a non-vanishing E_{nm}, we have to eliminate A_3 and the only way is to use A_2 to cancel it.

The condition $A_2+A_3=o(\delta^s)$ can be satisfied when $-n\delta-\beta\delta^s=0$, i.e.,

$$s=1,\quad \beta=-n. \tag{36}$$

The condition that $g\hat{J}_n(k_0R_1)+\hat{H}_n^{(1)}(k_0R_1)=0$ and Eq. (36) can be satisfied by different order multipoles. It is important to note that once the aforementioned two conditions are satisfied for a particular order, say n_0, they cannot be simultaneously satisfied by others orders. For $n=n_0$, we easily obtain that $E_{nm}=O(\delta^{n_0-2})$ and $A_{nm}=O(\delta^{2n_0-1})$; For $n\neq n_0$, we obtain from Case 1.1 that $E_{nm}=O(\delta^{n+1})$ and $A_{nm}=O(\delta^{2n+1})$. The behaviors of cloaking and shielding effect are different for various order of multipoles.

- Case of $n_0=1$: $E_{1m}=O(\delta^{-1})$ approaches infinity and $A_{1m}=O(\delta^1)$ approaches zero, which means the resonance mode. It is worth mentioning that the interior resonance does not destroy the cloaking effect, which is different from the conclusion of [12]. This difference is possibly due to the fact that [12] uses the Cauchy data, i.e., the mapping from the total field to its normal derivative, whereas this paper studies the mapping from the incidence field to the scattered one.
- Case of $n_0=2$: $E_{2m}=O(\delta^0)$ is in the same order as the incidence wave and $A_{2m}=O(\delta^3)$ approaches zero, which means sensor mode.
- Case of $n_0\geq 3$: Both E_{nm} and A_{nm} approach zero, which means ideal cloaking mode, i.e., cloaking effect and shielding effect are hand in hand.

From the condition of $g\hat{J}_n(k_0R_1)+\hat{H}_n^{(1)}(k_0R_1)=0$ and the definition of $g(\alpha)$ in Eq. (19), we easily obtain the value of α that leads to the resonance mode (for $n_0=1$) and the sensor mode (for $n_0=2$),

$$\alpha=\frac{\hat{J}_{n_0}'(k_0R_0)-\hat{Y}_{n_0}'(k_0R_0)\hat{J}_{n_0}(k_0R_1)/\hat{Y}_{n_0}(k_0R_1)}{\hat{J}_{n_0}(k_0R_0)-\hat{Y}_{n_0}(k_0R_0)\hat{J}_{n_0}(k_0R_1)/\hat{Y}_{n_0}(k_0R_1)}. \tag{37}$$

3.2. Case 2

When $\hat{J}_n'(k_0R_0)-\alpha\hat{J}_n(k_0R_0)=0$, we find that $E_{nm}=0$ and $\alpha=\hat{J}_n'(k_0R_0)/\hat{J}_n(k_0R_0)$. We carry out an analysis similar to that of Section 3.1, simply replacing $\left[g\hat{J}_n(k_0R_1)+\hat{H}_n^{(1)}(k_0R_1)\right]E_{nm}$ by $\hat{J}_n(k_0R_1)D_{nm}$. Thus, the necessary conditions for an electromagnetic wave to penetrate the inner boundary of the cloak are $\hat{J}_n(k_0R_1)=0$ and $f(R_1+\delta)=-n\delta+o(\delta)$ for a particular n_0. The resonance mode (for $n_0=1$) and the sensor mode (for $n_0=2$) are the same as those discussed in Section 3.1.

3.3. Removal of singularity

As shown in Section 3.1 and Section 3.2, one of the conditions for achieving the sensor mode is $f(R_1+\delta)=-n\delta+o(\delta)$. We note that the condition of zero scattering outside of the cloak

#151762 - $15.00 USD Received 27 Jul 2011; revised 7 Sep 2011; accepted 9 Sep 2011; published 3 Oct 2011

requires that $f(R_2) = R_2$. Thus, if $r' = f(r)$ is a continuous function, inevitably there is a particular value of r, say R_b, for which $r' = 0$. Consequently, from Eq. (12) we conclude that a singularity appears in the cloak layer since the argument for $H_n^{(1)}(\cdot)$ is zero. To remove such a singularity, we let the function f to be discontinuous at $r = R_b$, but at the same time, we keep the continuity of the permittivity and permeability. With this purpose, we see from Eqs. (4) and (5) that a function $f(r)$ that simultaneously satisfies $f(R_b^+) = -f(R_b^-) > 0$ and $f'(R_b^+) = f'(R_b^-)$ can achieve both the continuity of permittivity and permeability and the removal of singularity. One example of such f is depicted in Fig. 1.

It is interesting to discuss the meaning of the function $r' = f(r)$ for the case $r' < 0$. In deriving the permittivity and permeability in the physical space (Eqs. (4) and (5)), the key step is to use $x'/x = y'/y = z'/z = r'/r$ [3, 17]. When $r' < 0$, a point in the physical space and the corresponding point in the virtual space are on the opposite side of the origin. The invisibility conditions $f(R_1) = 0$ and $f(R_2) = R_2$ indicate that as we move from the inner boundary of the cloak to the outer one in the physical space, the corresponding point in the virtual space moves from the original to $r' = R_2$. However, since the virtual space is free space, there is no scattering at all. Consequently, it does not matter in which way we move from the original to $r' = R_2$ in the virtual space. The linear transform that is presented in [1, 17] indicates a uniform speed displacement. The concentrator transform that is presented in [3] indicates a displacement all the way outside of the outer boundary of the cloak, followed by a backward displacement to come back to the outer boundary. Here, in this paper, our transform function shows a displacement toward the opposite direction, followed a directional change and then a all-the-way displacement towards the outer boundary of the cloak.

4. Numerical simulations

Following the criteria that were presented in Section 3, we proposed a particular transformation, as depicted in Fig. 1(b), to test the performance of the cloaking device. We choose the following parameters: $R_0 = 0.5\lambda$, $R_1 = 1.5\lambda$, $R_2 = 3.0\lambda$, $R_a = 2.0\lambda$, $R_b = 2.33\lambda$, $R_c = 2.66\lambda$, and $h = 0.15\lambda$. The transform function in the range of $R_1 + \delta \le r \le R_2$ is given by

$$f(r) = \begin{cases} -n_0 r + n_0 R_1 & \text{for} \quad R_1 + \delta \le r < R_a \\ \frac{-h - n_0(-R_a + R_1)}{R_b - R_a}(r - R_a) + n_0(-R_a + R_1) & \text{for} \quad R_a \le r < R_b \\ \frac{-h - n_0(-R_a + R_1)}{R_b - R_a}(r - R_b) + h & \text{for} \quad R_b < r \le R_c \\ \frac{R_2 - n_0(R_a - R_1)}{R_2 - R_c}(r - R_c) + n_0(R_a - R_1) & \text{for} \quad R_c < r \le R_2. \end{cases} \tag{38}$$

We observe that the values of $\overline{\overline{\varepsilon}}$ and $\overline{\overline{\mu}}$ are both negative and finite in the region $R_1 + \delta \le r < R_a$, and the radial components approach zero at the boundary $r = R_1 + \delta$. In other regions, both $\overline{\overline{\varepsilon}}$ and $\overline{\overline{\mu}}$ are positive and finite. It is important to stress that although four transformations are used in the region of $R_1 + \delta \le r \le R_2$, the potential, and consequently the electromagnetic field, is expressed in a single formula, Eq. (12). The surface impedance α is calculated through Eq. (37).

We consider an x-polarized plane wave with a unit amplitude $\mathbf{E}^{\text{inc}} = \hat{x}e^{ik_0 z}$ is incident upon the cloaking device along the z direction. Since the given incidence wave contains only the $|m| = 1$ term, from here onwards, we drop off the m in the subscript for simplicity. For example, the coefficient K_{nm} is written as K_n. It is well known that K_n is proportional to $i^n(2n+1)/[n(n+1)]$ for both TE and TM components of the incident plane wave [3]. We aim at examining the cloaking effect and penetrating effect of the cloaking device as the parameter δ approaches zero. The cloaking effect is quantified by $|A_n/K_n|$. The lower the value of $|A_n/K_n|$, the better the cloaking effect. Since Eq. (19) shows that E_n/D_n is independent of δ, we can use only $|D_n/K_n|$

#151762 - $15.00 USD Received 27 Jul 2011; revised 7 Sep 2011; accepted 9 Sep 2011; published 3 Oct 2011

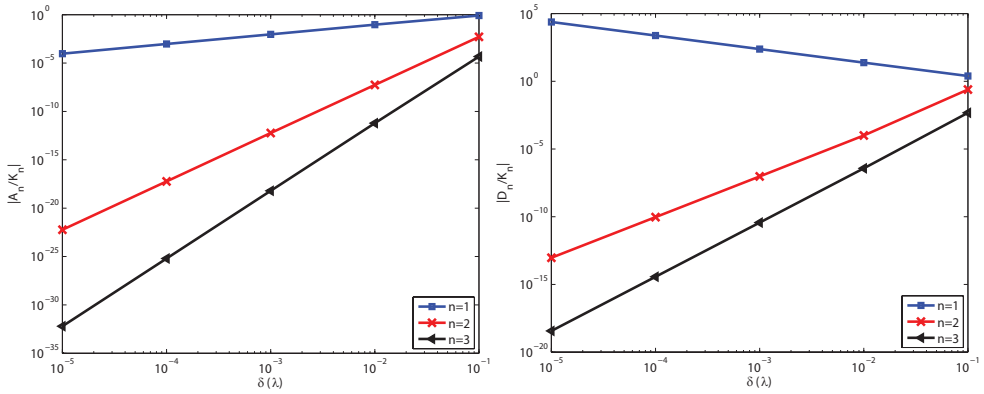

Fig. 2. For $n_0 = 1$, the cloaking and penetrating effects for different orders of multiples in the limit of δ approaching zero. (a) The cloaking effect. (b) Penetrating effect.

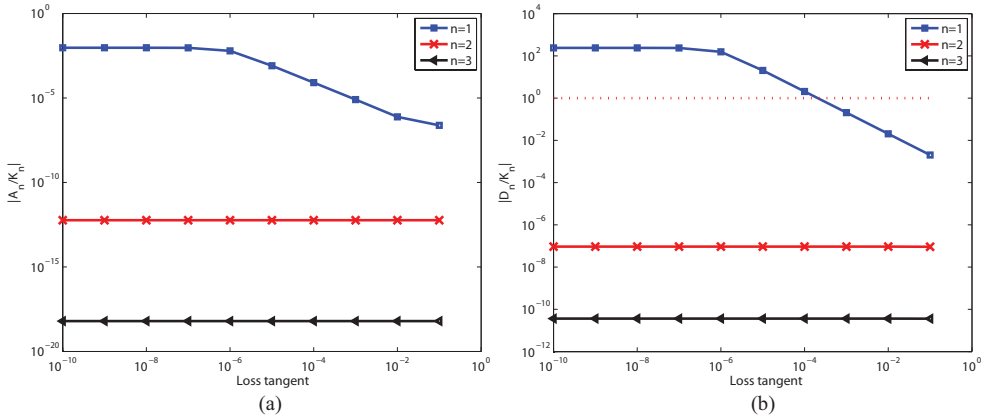

Fig. 3. For $n_0 = 1$ and $\delta = 10^{-3}$, the effect of surface impedance loss on the cloaking and penetrating effects. (a) The cloaking effect. (b) Penetrating effect, where the horizontal dotted line denotes the sensor mode.

to quantify the penetrating effect. The lower the value of $|D_n/K_n|$, the poorer the penetrating ability. The case of $|D_n/K_n| \gg 1$ corresponds to the resonance effect.

First, we let $n_0 = 1$. The quantities of $|A_n/K_n|$ and $|D_n/K_n|$ for different values of the small parameter δ and order number n are shown in Fig. 2. We see from Fig. 2(a) that the cloaking effect applies to all orders, including $n = n_0 = 1$. In addition, the slopes of the curves, which are in the logarithmic scale, agree with the theory presented in Section 3. That is to say, whenever δ is decreased by a factor 10, the values of $|A_n/K_n|$ decreases by a factor of 10, 10^5, and 10^7 for $n = 1$, $n = 2$, and $n = 3$, respectively. We see from Fig. 2(b) that the resonance effect applies to the order $n = n_0 = 1$ and the shielding effect applies to $n = 2$ and $n = 3$. In addition, the slopes of the curves agree with the theory, i.e., whenever δ is decreased by a factor 10, the values of $|D_n/K_n|$ increase by a factor of 10 for $n = n_0 = 1$ and decreases by a factor of 10^3 and 10^4 for $n = 2$ and $n = 3$, respectively. To summarize, for $n_0 = 1$, the wave component corresponding to $n = n_0$ yields resonance effect without external scattering, whereas the wave component corresponding to $n \neq n_0$ simultaneously yields cloaking and shielding effect.

#151762 - $15.00 USD Received 27 Jul 2011; revised 7 Sep 2011; accepted 9 Sep 2011; published 3 Oct 2011

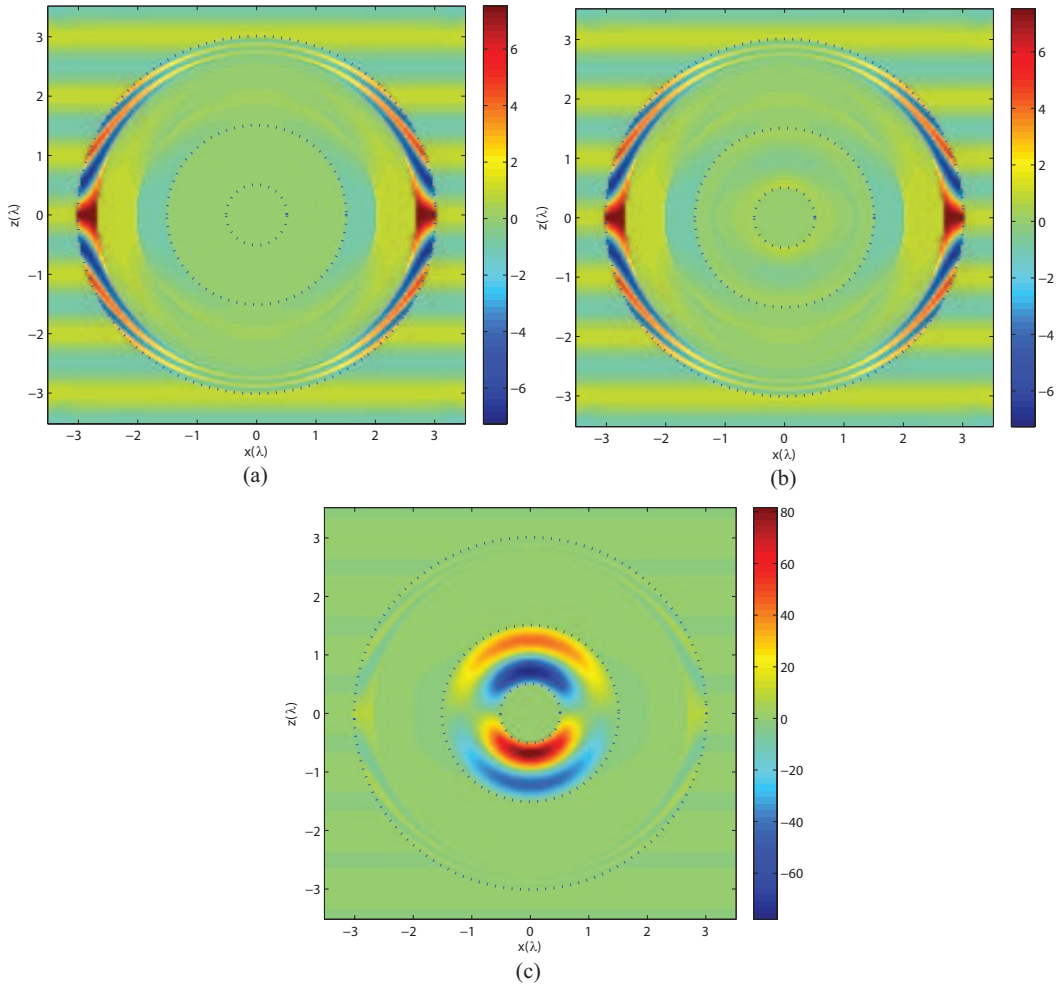

Fig. 4. For $n_0 = 1$, the x component of the electric field in the xz plane for the loss tangent of (a) 10^{-2}, (b) 10^{-4}, and (c) 10^{-7}, corresponding to the ideal cloaking, sensor, and resonance mode, respectively.

Since the sensor surface will result in some energy loss, we are interested in analyzing how this loss affects the cloaking and penetrating. To this purpose, we calculate $|A_n/K_n|$ and $|D_n/K_n|$ in the case when the real surface impedance α is replaced by a complex one $\alpha(1+iL_t)$, where L_t denotes loss tangent. Fig. 3 depicts the values of $|A_n/K_n|$ and $|D_n/K_n|$ for $\delta = 10^{-3}$ for the range of loss tangent from 10^{-10} to 10^{-1}. Fig. 3(a) and (b) show that the loss enhances the cloaking effect and at the same time decreases the penetrating effect for the order $n = n_0 = 1$, but it barely affects the cloaking or penetrating effect for other orders. We see from Fig. 3(b) that for $n = n_0 = 1$, as the loss decreases, the penetrating ability changes from the shielding mode (i.e., ideal cloaking mode) to the sensor mode and then to the resonance mode. It is interesting to see that a moderate loss, such as loss tangent of 10^{-4}, is able to enhance the cloaking effect and at the same time to shift the resonance mode to the sensor mode. In Fig. 4, we plot the x component of the electric field in the xz plane for the loss tangent of 10^{-2}, 10^{-4}, and 10^{-7}, corresponding to the shielding (i.e., ideal cloaking), sensor, and resonance mode, respectively.

#151762 - $15.00 USD Received 27 Jul 2011; revised 7 Sep 2011; accepted 9 Sep 2011; published 3 Oct 2011

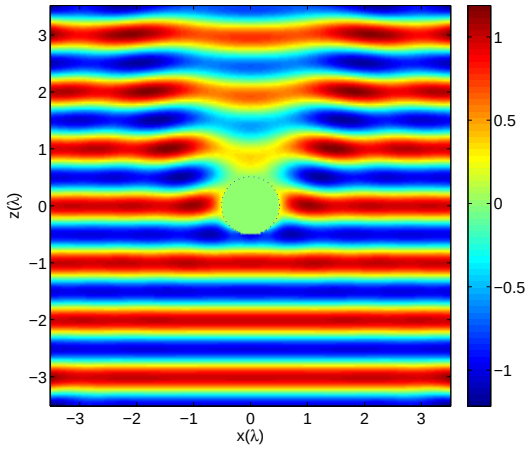

Fig. 5. The x component of the electric field in the xz plane for the case when only the sensor exists, without the presence of the outer cloaking layer.

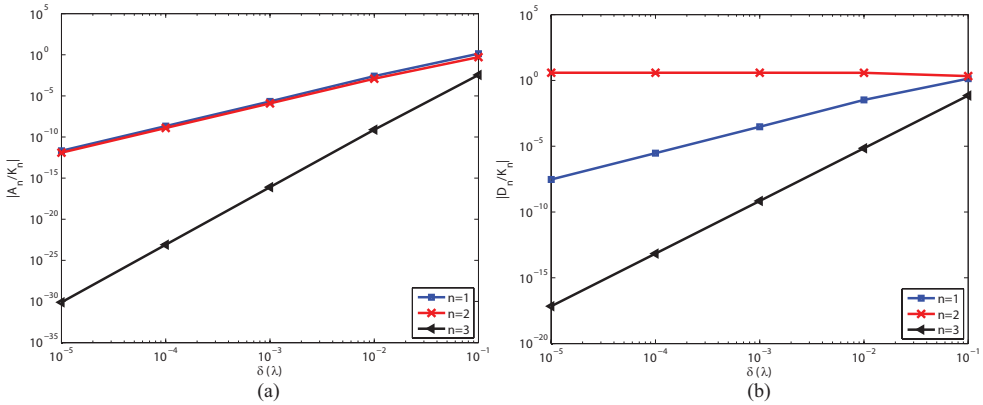

Fig. 6. For $n_0 = 2$, the cloaking and penetrating effects for different orders of multiples in the limit of δ approaching zero. (a) The cloaking effect. (b) Penetrating effect.

In comparison,when only the sensor exists, without the presence of the outer cloaking layer, the distribution of the electric field is plotted in Fig. 5, where we see that the distorted field pattern indicates the presence of a scatterer.

Next, for $n_0 = 2$, we also analyze the cloaking and penetrating effects. We see from Fig. 6(a) that the cloaking effect applies to all orders, including $n = n_0 = 2$ and the slopes of the curves agree with the theories, i.e., whenever δ is decreased by a factor 10, the values of $|A_n/K_n|$ decreases by a factor of 10^3, 10^3, and 10^7 for $n = 1$, $n = 2$, and $n = 3$, respectively. We see from Fig. 6(b) that the sensor mode applies to the order $n = n_0 = 2$ and the shielding effect applies to $n = 1$ and $n = 3$. The slopes of the curves agree with the theory, i.e., whenever δ is decreased by a factor 10, the values of $|D_n/K_n|$ keeps the same order for $n = n_0 = 2$ and decreases by a factor of 10^2 and 10^4 for $n = 1$ and $n = 3$, respectively. To summarize, for $n_0 = 2$, the wave component corresponding to $n = n_0$ yields sensor effect without external scattering, whereas the wave component corresponding to $n \neq n_0$ simultaneously yields cloaking and shielding effects. Fig. 7 depicts the values of $|A_n/K_n|$ and $|D_n/K_n|$ for $\delta = 10^{-3}$ for presence of loss

#151762 - $15.00 USD Received 27 Jul 2011; revised 7 Sep 2011; accepted 9 Sep 2011; published 3 Oct 2011

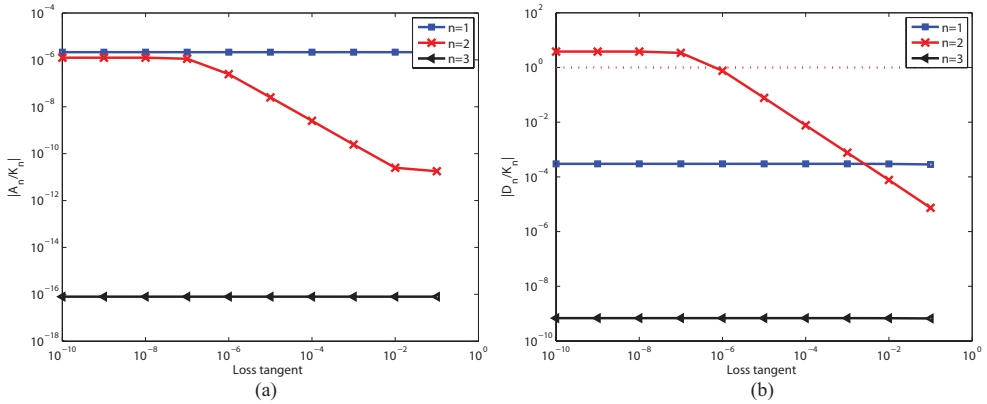

Fig. 7. For $n_0 = 2$ and $\delta = 10^{-3}$, the effect of surface impedance loss on the cloaking and penetrating effects. (a) The cloaking effect. (b) Penetrating effect, where the horizontal dotted line denotes the sensor mode.

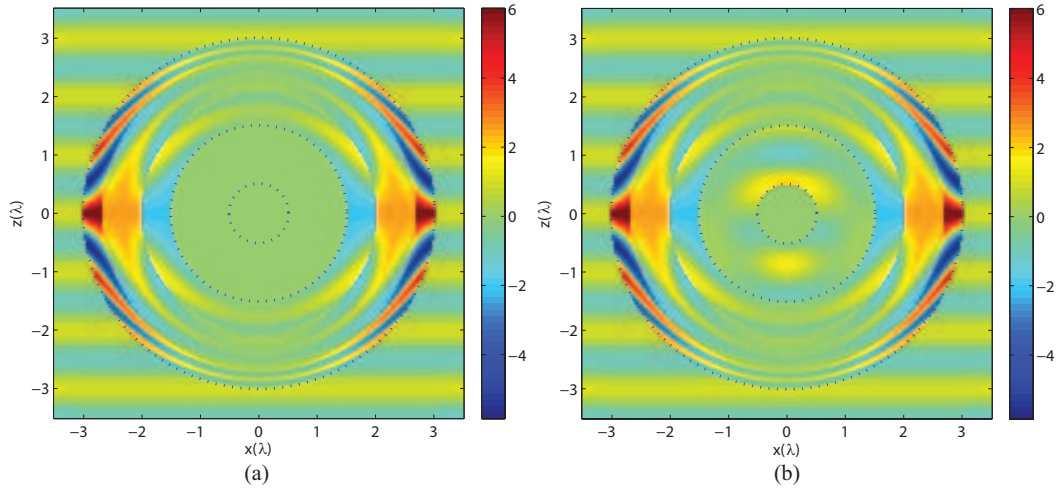

Fig. 8. For $n_0 = 2$, the x component of the electric field in the xz plane for the loss tangent of (a) 10^{-4} and (b) 10^{-7}, corresponding to the ideal cloaking and sensor mode, respectively.

in the surface impedance. We observe that the loss enhances the cloaking effect and in the meanwhile decrease the penetrating effect for the order $n = n_0 = 2$, but it barely affects the cloaking or penetrating effect for other orders. We see from Fig. 7(b) that for $n = n_0 = 2$, as the loss decreases, the penetrating ability changes from the shielding mode to the sensor mode. In Fig. 8, we plot the x component of the electric field in the xz plane for the loss tangent of 10^{-4} and 10^{-7}, corresponding to the shielding and the sensor mode, respectively. In practice, for $n = n_0 = 2$, the sensor mode can easily be destroyed by the loss. For example, in Fig. 8 a loss tangent of 10^{-4} is able to shift the sensor mode to the shielding mode.

5. Conclusion

The ideal transformation optics cloaking is accompanied by shielding: external observations do not provide any indication of the presence of a cloaked object, nor is any information about the

#151762 - $15.00 USD Received 27 Jul 2011; revised 7 Sep 2011; accepted 9 Sep 2011; published 3 Oct 2011

fields outside detectable inside the cloaked region. In this paper, we proposed a transformation that cloaks three-dimensional objects for electromagnetic waves in sensor mode, i.e., cloaking accompanied by degraded shielding. The proposed transformation tackles the difficulty caused by the fact that the lowest multipole in three-dimensional electromagnetic radiation is dipole rather than monopole. It is worth emphasizing that we have obtained the analytical solution to the electromagnetic fields in each region of the whole space. We find that for the dipole term (n=1), we are able to achieve resonance mode without external scattering. For the quadrupole term (n=2), we are able to achieve sensor mode without external scattering. However, the loss that is presented on the surface of the sensor degrades the penetrating effect so that a moderate loss is able to shift the resonance mode to the sensor mode for $n = 1$ and to shift the sensor mode to the ideal cloaking mode for $n = 2$. Thus, in real world applications, where loss is present on the surface of sensor, it is more desirable to achieve the sensor mode using the dipole term.

Acknowledgement

The author Chen acknowledges the financial support from the Singapore Temasek Defence Systems Institute under grant TDSI/09001/1A.

#151762 - $15.00 USD Received 27 Jul 2011; revised 7 Sep 2011; accepted 9 Sep 2011; published 3 Oct 2011